Eur Biophys J (2005) 34: 344–352
DOI 10.1007/s00249-004-0456-6

ARTICLE

U. Lehnert · V. Réat · G. Zaccai
D. Oesterhelt

Proton channel hydration and dynamics of a bacteriorhodopsin triple mutant with an M-state-like conformation

Received: 16 August 2004 / Revised: 30 November 2004 / Accepted: 5 December 2004 / Published online: 2 February 2005

Abstract The hydration and dynamics of purple membranes (PM) containing the bacteriorhodopsin (BR) triple mutant D96G/F171C/F219L were investigated by neutron diffraction coupled with H_2O/D_2O exchange and by energy-resolved neutron scattering. The mutant, which is active in proton transport (Tittor et al. in *J. Mol. Biol.* 319:555–565, 2002), has an 'open' ground-state structure similar to that of the M intermediate in the photocycle of the wild type (wt) (Subramaniam and Henderson in *Nature* 406:653–657, 2000). The experiments demonstrated an increased proton channel hydration in the mutant PM compared with wt PM, in both high (86%) and low (57%) relative humidity. We suggest that this is due to the smaller side chains of the mutant residues liberating space for more water molecules in the proton channel, which would then be able to participate in the proton translocation network. PM thermal dynamics has been shown to be very sensitive to membrane hydration (Lehnert et al. in *Biophys. J.* 75:1945–1952, 1998). The global dynamical behaviour of the mutant PM on the 100-ps time scale, as a function of relative humidity, was found to be identical to that of the wt, showing that the 'open' BR structure and additional water molecules in the proton channel do not provide a softer environment enabling increased flexibility.

Keywords Incoherent neutron scattering · Neutron diffraction · Mean square amplitudes · Purple membranes · Hydration

U. Lehnert · D. Oesterhelt
Max-Planck-Institut für Biochemie,
82152 Martinsried, Germany

U. Lehnert · G. Zaccai
Institut Laue-Langevin, 156, 38042
Grenoble Cedex 9, France

U. Lehnert · G. Zaccai (✉)
Institut de Biologie Structurale Jean Pierre Ebel
CEA-CNRS-UJF, 38027 41 rue Jules Horowitz,
Grenoble Cedex 1, France
E-mail: zaccai@ibs.fr
Fax: +33-4-38785494

V. Réat
Institut de Pharmacologie et Biologie Structurale,
UMR 5089 CNRS-UPS,
31077 Toulouse, France

Introduction

Hydration is a dominant factor for the ability of a protein to undergo functional conformational changes as has been shown by studies on bacteriorhodopsin (BR), a heptahelical transmembrane protein (Sass et al. 1997; Weik et al. 1998b). In the purple membrane (PM) of the halophilic archeon *Halobacterium salinarum*, BR is organised with lipids on a two-dimensional crystal lattice (Blaurock and Stoeckenius 1971). The colour of PM is due to the chromophore, retinal, which is covalently bound to Lys216 in BR via a Schiff base linkage. Upon light absorption, the isomerisation of the retinal initiates a catalytic cycle leading to the unidirectional transport of a proton from the cytoplasm to the extracellular medium. The catalytic cycle is characterised by a photocycle of spectroscopic photointermediates denoted J, K, L, M, N, O (review in Haupts et al. 1999). The photointermediate M, is the longest lived and the only state in which the Schiff base is deprotonated. M has been divided into two substates, M1 and M2 (Váró and Lanyi 1990, 1991a). They differ by the accessibility of the Schiff base to either the extracellular or the cytoplasmic side of the membrane, respectively. The irreversible 'turning' of the Schiff base in the M1 to M2 transition is a necessary requirement for vectorial proton transport.

From numerous studies on wild-type (wt) and mutant BR molecules, which accumulate preferentially in the M or N states, it has been shown that large conformational changes occur in these intermediates (Dencher et al. 1989; Kamikubo et al. 1996; Koch et al. 1991; Luecke et al. 2000; Sass et al. 1997; Subramaniam et al. 1999;

Vonck 2000; Weik et al. 1998b), which, it has been suggested, might allow the entry of water molecules in the proton channel region. The particularity of the triple mutant, D96G/F171C/F219L, is that its ground-state structure as solved by electron microscopy displays all of the features seen in light-induced changes in wt BR (Subramaniam and Henderson 2000). The mutant is active in proton transport and, unlike wt BR, has been shown to undergo only minor structural changes during its photocycle (Tittor et al. 2002).

Neutron diffraction, X-ray and Fourier transform IR (FTIR) measurements have revealed several water molecules inside BR, which have been proposed to play a crucial role in the proton translocation mechanism (review by Dencher et al. 2000). Neutron diffraction coupled with H_2O/D_2O exchange is a direct means to investigate the hydration of the proton channel at low resolution. It is a low-resolution diffraction method, which is sensitive to all water molecules present in the structure and not only to the ones that are ordered to high resolution as is the case for X-ray crystallography. Four tightly bound water molecules have been identified by neutron diffraction to remain in the proton channel even in completely dried ground-state BR (Papadopoulos et al. 1990). The M state, cryo-trapped in the D96N BR mutant, has not revealed major changes in hydration in the proton channel projection compared with its ground state (Weik et al. 1998b). High-resolution X-ray crystallography structures of the ground state have identified a water network of seven to eight molecules in the extracellular half of the protein (Luecke et al. 1999; Pebay-Peyroula et al. 1997). It has been suggested that the M conformation might cause increased hydration of the cytoplasmic domain (Cao et al. 1991) and hydrostatic pressure measurements have revealed a volume change of the protein during the photocycle, which was related to hydration changes (Váró and Lanyi 1995). FTIR measurements have indicated that internal water molecules are relocated during the photocycle, and three additional water molecules have been suggested as likely to facilitate proton transfer between Asp96 and the Schiff base in the cytoplasmic domain (Maeda et al. 2000; Sass et al. 2000).

Local and global dynamic fluctuations play an important role in protein function and activity (Karplus and McCammon 1983). Incoherent neutron scattering is an especially powerful tool for the investigation of angstrom-level fluctuations in the picosecond to nanosecond time range. Measured parameters in this length–time scale reflect the motions of amino acid side chains, which also act as the lubricant for larger conformational changes on the millisecond time scale (Gabel et al. 2002; Kneller and Smith 1994; Smith 1991). Neutron scattering experiments on PM have revealed the hydration dependence of the dynamics and dynamical transitions from harmonic to nonharmonic regimes at temperatures between 150 and 250 K (Ferrand et al. 1993; Lehnert et al. 1998; Réat et al. 1996). These findings have led to establishing a correlation between BR activity and thermal motions following the earlier hypothesis (Zaccai 1987) that the membrane protein required a soft global environment obtained through lipid headgroup hydration and temperature. A further correlation has been established between dynamics and BR function as a membrane pump, by neutron scattering experiments on specifically labelled PM, which showed that the retinal binding pocket and extracellular half of the protein constituted a dynamically harder, less flexible, core as would be expected for a pump valve that ensures unidirectional flow (Réat et al. 1998). The more resilient environment would act as a better control of the change in Schiff base orientation during the M1 to M2 transition in the photocycle. Function-related heterogeneous dynamics within the BR structure has also been shown for much slower time scales (on the 10-Hz frequency scale) by solid state NMR (Kira et al. 2004).

In this paper, we report results in the context of dynamics-hydration-function and structure relations. We took advantage of the 'open' structure of the triple mutant in its ground state at room temperature (in contrast to earlier studies on mutants, which required low temperature for trapping this particular structure) in order to compare its proton channel hydration with that in the ground state of wt BR. The increased proton channel hydration observed in the mutant is discussed in terms of the mutated amino acid side chains occupying a smaller volume. The dynamics of the triple mutant measured for different relative humidity (rh) values was found to be identical to that of the wt, suggesting that the additional water molecules are confined in the structure of BR and thus do not alter the internal flexibility of the protein.

Materials and methods

Sample preparation

PM containing triple mutant BR-D96G/F171C/F219L or wt BR was isolated from cells according to the standard procedure described by Oesterhelt and Stoeckenius (1974). PM samples containing either triple mutant or wt BR were prepared simultaneously.

For neutron diffraction experiments, 90–100 mg of concentrated triple mutant and wt PM suspension in H_2O was deposited on both faces of ten quartz slides ($63\times9\times0.5$ mm^3, Suprasil 300, Hellma, Müllheim, Germany), respectively. Slow drying of the membranes over several days in a dessicator at a rh of 86% in H_2O led to oriented membrane fragments parallel to the slides with a rotational in-plane disorder. The quartz slides were stacked and mounted in a special sample holder before the neutron diffraction measurements. The sample holder, allowing two samples to be kept in the same environment, was placed in a closed temperature-controlled humidity chamber. The rh in the chamber was defined by placing appropriate saturated salt solutions in

H_2O or D_2O [KCl for 86% and NaBr for 57% rh (O'Brien 1948)] and maintaining the temperature at 20°C.

For incoherent neutron scattering experiments, an aqueous suspension of purified PM was washed three times in D_2O by centrifugation for 60 min at 100,000*g* at 10°C. The pellet of PM was resuspended in D_2O and homogenised in a potter. The volume ratio between the PM pellet and D_2O was about 1:20. After three resuspension-centrifugation steps the H_2O and labile H atoms in the sample were considered as fully exchanged. After the last centrifugation step, the D_2O-washed pellet (200–250 mg PM) was layered in an aluminium sample holder (dimensions 4×3 cm^2, height 0.5 mm). Rapid, partial drying was achieved with silica gel in a desiccator at room temperature until the final D_2O content reached about 0.5 mg mg^{-1} PM (measured by weighing). Final equilibration to the required hydration level was achieved by replacing the silica gel by a saturated solution of an appropriate salt in D_2O; this precisely defined the rh. The salts were NaBr for 57%, NaCl for 75%, KCl for 86% and KNO_3 for 93% rh (O'Brien 1948). The dry sample was obtained by complete desiccation over silica gel. Each equilibration proceeded for 7–9 days, until the weight of the sample and sample holder did not vary by more than 0.3 mg per day. The sealed sample holder was placed in a cryostat during the neutron diffraction experiments and its weight was checked before and after the experiment to verify its tight sealing. Once the experiments had been accomplished, the total amount of water in the sample was estimated by weighing before and after complete drying over silica gel.

Neutron diffraction experiments

Measurements were carried out at the Institute Laue-Langevin (ILL, Grenoble, France) on the diffractometer D16 at a wavelength of $\lambda = 4.5$ Å and in a Q range of [0.05;2.4] $Å^{-1}$. The measuring time per sample in a H_2O or a D_2O atmosphere was about 3 days. The lamellar diffraction of the membrane stacking was measured to check the stability of the hydration state and to monitor the equilibration of the sample. The intensity of the (h,k) reflections of the hexagonal PM lattice were recorded by moving the detector stepwise from $\gamma = 7°$ to 40° with a step of 0.29°. The sample was rotated at the same time by $\omega = \gamma/2$ around its axis to ensure a constant path length through the sample.

The recorded powder intensities were reduced as described previously (Jubb et al. 1984; Weik et al. 1998b) to obtain structure factors. The normalised integrated intensities were split according to their ratio determined by electron diffraction (Henderson et al. 1986; Henderson and Unwin 1975) and Lorentz-corrected. In order to compensate for differences in measured effective masses and for changes in sample alignment in the neutron beam of the different data sets of wt and mutant PM samples the corrected intensities were calibrated. A normalisation factor n was established in the respective H_2O measurement for the sum of the reflection from (1,1) to (5,2) and then applied to the D_2O data: $\sum_{h,k} I_{\text{sample1}}(h,k) = n \sum_{h,k} I_{\text{sample2}}(h,k)$. The (1,0) reflection was omitted to avoid partial contamination by the lamellar reflection of the membrane stacking. This procedure allowed a direct comparison of the following calculated Fourier maps, because the structural changes in the triple mutant compared with the ground-state wt structure do not alter the total cross section of the elementary cell. Applying a scaling factor to the corrected intensities of the data sets, we compensated a different sample alignment in a H_2O and D_2O atmosphere. From previous measurements, the mean value of the ratio $\sum_{h,k} I_{D_2O}(h,k) / \sum_{h,k} I_{H_2O}(h,k)$ of the corrected intensities for one sample at a defined rh state was calculated and applied to the data sets concerned as described previously (Weik et al. 1998b). A 5% variation of the scaling factor did not affect the projected proton channel hydration difference of wt and triple mutant BR molecules.

Structure factor phases for the difference Fourier maps were taken from electron microscopy (Henderson et al. 1986). The projection Fourier maps were put on an absolute scale by using the contours of helix B in the density map of PM in H_2O (Zaccai and Gilmore 1979). The coherent scattering length of helix B was calculated from its amino acid composition and amounts to $b_{\text{helix B}} = 57.2 \times 10^{-12}$ cm. The mean scattering length for two lipid molecules spanning the membrane is $b_{\text{lipid}} = 10 \times 10^{-12}$ cm. In this calculation it was taken into account that the lipid composition of the extracellular part differs from that of the intracellular part (Kates et al. 1982) and that the signal in the projection maps corresponds to two lipids. Thus, a scattering length b_{cal} per square angstrom can be assigned to the contours:

$$b_{\text{cal}} = \frac{b_{\text{helixB}} - b_{\text{lipid}}}{C_B A_{\text{helix}} + C_L A_{\text{lipid}}}$$

where C_B is the mean contour level of helix B in the density map in H_2O, $A_{\text{helix}} = 75$ $Å^2$ is the projected helix area, C_L is mean negative lipid contour level in the density map in H_2O and $A_{\text{lipid}} = 69$ $Å^2$ is the projected area of a lipid molecule.

Elastic incoherent neutron scattering experiments

Elastic incoherent scattering reflects the displacement of individual atoms on the nanosecond to picosecond time scale, depending on the energy resolution of the spectrometer. The decrease of the elastic scattered neutron intensity as a function of increasing temperature indicates the onset of vibrational (inelastic scattering) and diffusive (quasielastic scattering) motions. At a given temperature T the elastic scattering function $S(Q,\omega = 0)$ in the Gaussian approximation is given by $S_{\text{inc},T}(Q, \omega = 0) = A \exp\{-\langle u^2 \rangle / 6 \cdot Q^2\}$, where the mean

square amplitudes $<u^2>$ correspond to the full elongation of atomic displacement in the time window of the experiment and A is a constant. The Gaussian approximation is valid in the case of harmonic vibrations or in a region where $Q\sqrt{\langle u^2\rangle/2}\leqslant 1$, which is similar to the Guinier formalism for small-angle scattering (Réat et al. 1996). In practice, it is valid for a trajectory that is localised within a distance of $1/Q$ or less in a time of t or less of the measurement time window.

The incoherent neutron scattering experiments were performed on the backscattering instruments IN16 (energy resolution $\Delta E = 1$ μeV, $\lambda = 6.275$ Å) and IN13 ($\Delta E = 8$ μeV, $\lambda = 2.23$ Å) at the ILL. Sample containers were placed in a cryostat with an orientation of 135° between the incident neutron beam and the sample plane and taken to 20 K at a rate of 2 K min^{-1}. Data were collected on the triple mutant and the wt on IN16 for 15 min every 3 K from 20 to 320 K. On IN13, the collection time was set at 20 min for temperatures up to 200 K, after which the counting time was doubled. The chosen temperature step width was 5 K. Normalised intensities were corrected for scattering by the empty sample container and for absorption, which takes the orientation of the sample holder into account. The normalisation to the detector efficiency was done with the measurement of the sample itself taken at the lowest temperature where an essentially wave-vector, **Q**, independent scattering pattern is expected. Angles on which Bragg reflections of the aluminium sample holder appear were discarded in the further analysis. The corrected data were grouped to an averaged temperature step of 10 K. The mean square amplitudes $<u^2>$ at a given temperature T were calculated according to the Gaussian approximation from a linear fit of $\ln\{I_T(Q,\omega=0)/I_{T_0}(Q,\omega=0)\}$ as a function of Q^2. High-amplitude motions were extracted from IN16 in a wave-vector range $Q = [0.43;1.25]$ Å^{-1} and small-amplitude motions were calculated from $Q = [1.99;3.76]$ Å^{-1} on IN13. The error evaluation of the linear fit (and therefore on $<u^2>$) assumed weighted statistical errors around each intensity data point, and was calculated in the graphics program Igor (Igor Pro, version 4.3, WaveMetrics). The $<u^2>$ values were then plotted as a function of absolute temperature T.

Force constants $<k>$ were calculated from the $<u^2>$ versus temperature T plots (Zaccai 2000). They were defined as resilience values and calculated as $\langle k\rangle = 2k_B/\left(\mathrm{d}\langle u^2\rangle/\mathrm{d}T\right)$, with the Boltzmann constant $k_B = 1.38\times10^{-23}$ J K^{-1} and $(\mathrm{d}<u^2>/\mathrm{d}T)$ expressed in metres squared per Kelvin.

Results

Hydration of triple mutant and wt PM

Structure factors were calculated from in-plane neutron diffraction measurements in D_2O and H_2O atmospheres of different rh for each PM type, and were calibrated as described in Materials and methods. Difference (D_2O minus H_2O) Fourier maps, calculated from these data, displayed the exchangeable hydrogen atoms and water molecules in the in-plane membrane projection (Figs. 1, 2). We recall the zero contour level in a difference Fourier map represents the mean scattering density level in the unit cell, and positive and negative contours represent density differences with respect to this mean.

In the 86% rh maps, several prominent exchangeable H or hydration peaks are present in the lipid and proton channel regions of the membrane. Three different hydration sites can be distinguished arising from hydration of the lipid head groups (Zaccai and Gilmore 1979). There is a feature in the intra-trimer region, where one of the glycolipid sulphate molecules was located by neutron diffraction (Weik et al. 1998a), the second one is in the inter-trimer region and the third one appears between helices A, G and E of adjacent BR molecules. The hydration peak in the interior of the protein arises from the exchangeable protons and water molecules in the proton channel (Papadopoulos et al. 1990). The princi-

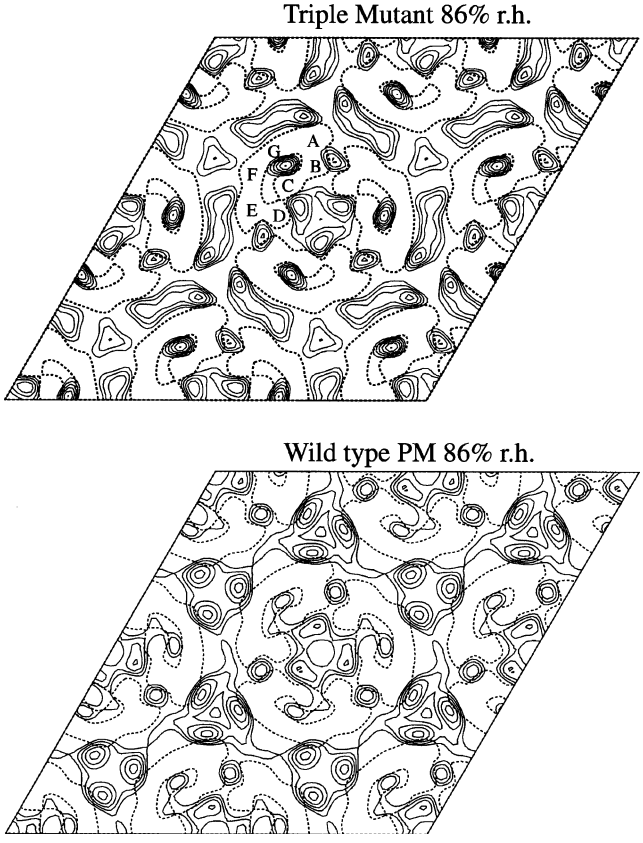

Fig. 1 D_2O–H_2O difference Fourier maps at 86% relative humidity (*rh*) of triple mutant and wild-type (*wt*) purple membranes (*PM*). Only positive contours are drawn in *continuous lines*. The outline of a bacteriorhodopsin (*BR*) monomer is drawn in *bold dashed lines* and the helix positions are indicated (*A–G*). Contour levels are equidistant and identical in both maps; the zero line was omitted. The lattice constant a was determined to be 62 Å

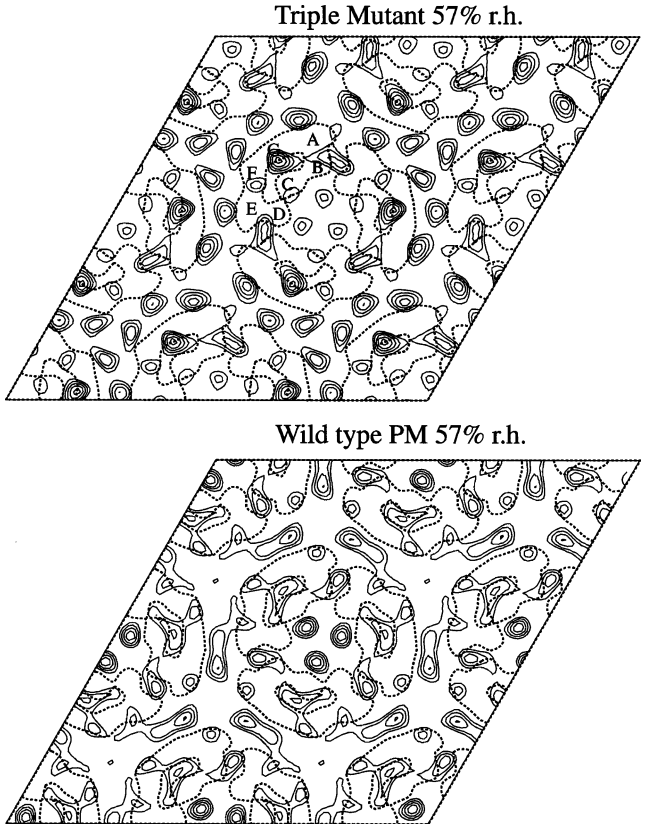

Fig. 2 D_2O–H_2O difference Fourier maps at 57% rh for the triple mutant and wt PM. Only positive contours are drawn in *continuous lines*. The outline of a BR monomer is drawn in *bold dashed lines* and the helix positions are indicated (*A–G*). Contour levels are equidistant and identical in both maps; the zero line was omitted. The lattice constant is $a = 61.4$ Å

pal characteristics of the maps are similar for mutant and wt PM. Significant differences occur, however, with respect to the area covered and the maximum contour level of each feature. The mutant proton channel hydration peak, in particular, occupies a bigger area and rises to higher contour levels than in wt PM. Differences between the lipid headgroup hydration peaks in the mutant and wt maps may be due to a reorganisation of lipid molecules. The limitations of the difference Fourier method, however, and the inherent noise and sensitivity of the maps to phasing assumptions induce us to be very cautious before proposing such an interpretation.

Fewer hydration sites are visible in the difference Fourier maps at 57% rh. Hydration in the lipid regions has decreased with respect to 86% rh as water molecules were dried off from around the lipid headgroups. In the intra-trimer region higher contours are reached for wt PM, whereas in the inter-trimer region a higher level is observed for the triple mutant. The most intensive feature is situated in the proton channel of the triple mutant. It occupies a large area and is extended towards helix G compared with the feature at 86% rh. In wt PM, also, the channel hydration peak is spread out into a larger area in the drier membrane.

Proton channel hydration of triple mutant and wt BR

The difference Fourier maps for the mutant and wt samples at each of 86 and 57% rh can be compared directly as the contour levels were chosen at the same values. The area enclosed by a contour level in the maps was approximated by that of an ellipse. The scattering volume represented by a proton channel peak was estimated as that of a number of stacked elliptical cylinders. The base line was set to the mean negative level located in the protein area of the difference map where the density of exchangeable H atoms is expected to be a minimum and to have the same value for mutant and wt membranes. Such an approximation cannot be avoided because, as usual in crystallography, the technique does not permit us to determine the experimental $F(0,0)$ structure factor from the data. The results of the calculation are listed in Table 1. The hydration volume in the channel for each sample is similar for 86 and 57% rh. The volume and the maximum contour value for the triple mutant, however, are about twice the values for wt PM, which is clearly outside the errors. Moreover, partial drying of the membranes to 57% rh does not affect the difference in the channel hydration between wt and mutant. The scattering volumes can be put on an absolute scale by calibrating against the B-helix feature in the projection density map of wt PM in H_2O (Zaccai and Gilmore 1979). This calculation leads to 7 ± 2 more protons in the channel of the triple mutant compared with wt BR. It can be excluded that this difference arises from the mutated amino acids, because the number of exchangeable hydrogens is not altered by the mutation. The difference in the number of exchanged protons in the channel projection corresponds to an excess of about four water molecules.

The present study can be compared directly with previous neutron diffraction studies on hydration such

Table 1 Calculated scattering volume and maximum contour level of the hydration channel from the difference Fourier map of triple mutant (*TRI*) and wild-type (*wt*) purple membranes at 86 and 57% relative humidity (*rh*)

Volume (Å^2×contour)				Maximum contour			
86% rh		57% rh		86% rh		57% rh	
TRI	wt	TRI	wt	TRI	wt	TRI	wt
6.1	2.5	7.6	2.9	5	2	5	3

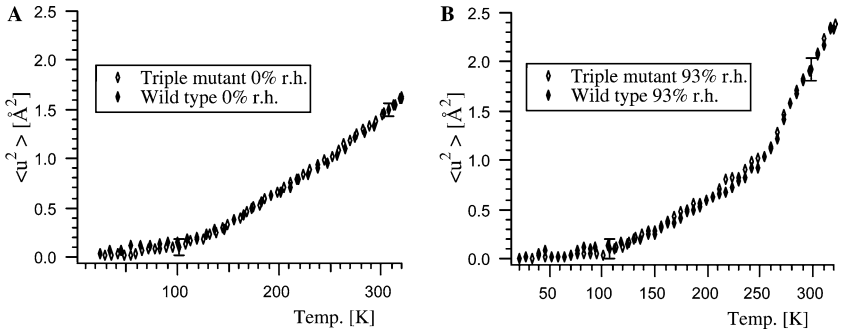

Fig. 3 High mean square amplitudes of the triple mutant (*open symbols*) and wt PM (*closed symbols*) for dry (**a**) and hydrated (**b**) membranes, measured on IN16 (see text). The same Q range was investigated in both types of sample. *Error bars* are only shown at two different temperatures

as that of Papadoulos et al. (1990) and the study of Weik et al. (1998b) on the M state cryo-trapped in the D96N mutant. The diffraction measurements were performed under identical conditions, on the same neutron diffractometer, and the data treatment followed the same protocol. Diffraction patterns were recorded on the M state of the D96N mutant of BR cryo-trapped from 86, 75 to 57% rh. Structural differences with the ground state, observed for the 86 and 75% rh samples, were absent in the 57% rh sample, suggesting that the state trapped at 57% rh was M1 and that M2 was trapped at the higher rh values. However, in contrast to the triple mutant data, which showed an increase of about four water molecules in the proton channel with respect to wt BR, in the case of the ground and M states of D96N the difference Fourier projections of exchangeable hydrogen atoms and water molecules in the membrane plane were identical within the 20% measurement error. The observation on D96N established that contrary to certain models, the wt structural changes in the M state were not correlated with major hydration changes in the proton channel projection.

Thermal motions of triple mutant PM and wt PM

Mean square fluctuation amplitudes, $<u^2>$, as a function of temperature, for wt and mutant PM under different rh conditions, are plotted in Figs. 3 and 4. They were calculated from neutron scattering measurements at different wave-vector ranges and energy resolution, corresponding to different length and time scales. The $<u^2>$ values correspond to the full elongation of atomic displacement in the time window of the experiment. As the experimental wave vector **Q** is proportional to the inverse of the length scale, the $<u^2>$ values from the low-Q range, $Q=[0.43;1.25]$ Å^{-1}, were called 'high-amplitude motions' and the ones from the high-Q range, $Q=[1.99;3.76]$ Å^{-1}, were called 'small-amplitude motions'. Dynamical characteristics of the mutant membrane were compared with motions found in wt PM. In their respective dynamical regimes, the general behaviour of the $<u^2>$ values, the dynamical transition temperatures as well as the hydration behaviour are identical for both types of membrane.

Figure 3 shows the high-amplitude $<u^2>$ of wt and triple mutant PM at the two extreme hydration states of 0 and 93% rh, on the 1-ns time scale. The $<u^2>$ as a function of temperature curves can be divided into several parts. At low temperature, the $<u^2>$ values increase linearly in a harmonic motion regime until the first hydration-independent transition temperature at 130 ± 5 K. The second regime up to the dynamical transition at 250 ± 5 K also shows no hydration dependence. The transition at 250 K, which is absent for the dry membrane (0% rh), declares the onset of hydration-dependent motions.

In the case of small mean square amplitudes (on the 100-ps timescale), only one high hydration state has been measured, confirming the similarity of the dynamics between triple mutant and wt PM (Fig. 4). A dynamical transition was found at 230 ± 10 K. Previous measurements have shown that this transition is absent in dry wt membranes (Ferrand et al. 1993). The hydration dependence of the small mean square amplitudes has been investigated in detail (Lehnert et al. 1998). It has been shown that the dynamical transition occurs for rh values above 57%, with decreasing resilience reaching progressively higher mean square amplitude values as the rh is increased.

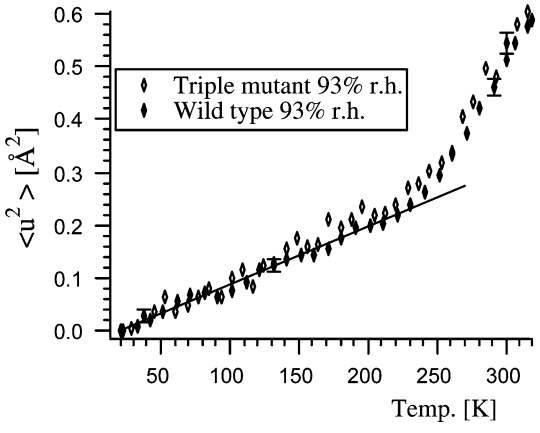

Fig. 4 Small mean square amplitudes at 93% rh of triple mutant (*open symbols*) and wt (*closed symbols*) membrane as derived from IN13 (see text). *Error bars* are only shown for two different temperatures. A linear fit through the harmonic region is shown and corresponds to a force constant of 2.3 N m^{-1}

Discussion

We investigated the hydration and the thermal dynamics of the triple mutant in comparison with wt PM. The main results are that an increased hydration by several additional water molecules is observed in the proton channel of the triple mutant, but that this does not influence the global thermal dynamics of the membrane on the 1-ns time scale.

What is the origin of the increased channel hydration in the triple mutant? A high-resolution structure of the triple mutant is not available currently, and we feel it would be too speculative to compare the location and number of water molecules found by neutron diffraction with water accessibility model calculations applied to other high-resolution structures of BR. Mutations of course do not only modify a structure locally at the changed amino acid, and the 'space' occupied by a water molecule may vary enormously according to its hydrogen-bonding pattern. All three mutated amino acids in the mutant are smaller than the ones they replace in wt BR. The volume decrease due to these mutations can, therefore, be calculated by assuming no other structural changes with respect to the wt structure.

The volumes in solution of Asp (D) and Gly (G) are 111 and 60 $Å^3$, respectively (Zamyatin 1972). Phe (F) occupies 190 $Å^3$ and is replaced by the smaller Cys (C) and Leu (L), with volumes of 109 and 167 $Å^3$, respectively. The gain in volume for water molecules, therefore, is 156 $Å^3$, of which 59 $Å^3$ is for residue 96, 81 $Å^3$ for residue 171 and 27 $Å^3$ for residue 219. A water molecule in bulk water occupies around 30 $Å^3$, which leads to available space for five water molecules per BR or two molecules near Gly96, two to three near Cys171 and about one near Leu219, matching the value found in the difference Fourier map. These numbers may of course be larger or smaller because of local structural rearrangements as well as different packing of side chains, however, and Schobert et al. (2003) identified a network of three water molecules near residue 219 in the crystal structure of the unilluminated F219L mutant of BR, where the residue replacement obviously created a larger water-accessible cavity than the 27 $Å^3$ of the F to L side-chain volume difference.

The study of proton channel hydration in the D96N mutant suggested that the structural changes between the ground and M states, observed in both the mutant and wt BR, are not correlated with major hydration changes in the proton channel projection (Weik et al. 1998b). In the D96N mutant, the replacement of an Asp residue by Asn is isosteric and does not lead to a change in occupied volume or projected surface area of the residue, whereas the triple mutant amino acid changes lead to large changes in residue occupied volumes.

A movement of Phe219 in the late M-state (where the Schiff base is accessible to the cytoplasmic side) structure of wt BR has been reported to enlarge several cavities in the cytoplasmic domain (Sass et al. 2000). This supports the suggestion that the replacement of the Phe219 with a smaller residue favours an increase in the number of water molecules in the cytoplasmic region of BR. It has been suggested that the structural changes in the F219L mutant accumulating in the N state and showing structural changes similar to those of the triple mutant are large enough to allow several water molecules to enter the channel (Vonck 2000; Schobert et al. 2003) and several water molecules have been placed in the proton channel, including two near Asp96 and Val49 by FTIR spectroscopy (Kandori 2000). Several ordered water molecules are seen in the high-resolution X-ray crystallography structures of the ground-state and M intermediate. Nine internal water molecules have been localised in the ground-state structure (Belrhali et al. 1999; Luecke et al. 1999); seven are in the extracellular part of the channel and two in the cytoplasmic part. In the late M state there are still seven water molecules in the extracellular half, but six or seven water molecules become visible in the cytoplasmic part (Sass et al. 2000). There is no direct evidence, however, permitting us to decide if they result from an influx of water molecules in the M-state structure or if they become ordered in this intermediate and are thus visible in the crystallographic structure.

Our results clearly indicated that the high- and small-amplitude thermal motions of PM containing triple mutant or wt BR are essentially identical. The additional water molecules in the channel do not alter the observed dynamical behaviour of the membrane. The influence of hydration changes on the $< u^2 >$ values has been studied in detail and was revealed to be an important parameter for BR function (Ferrand et al. 1993; Lehnert et al. 1998). A dynamical transition for the small- and high-amplitude motions at 230 and 250 K, respectively, was only observed for hydrated membranes. In these cases an increase in the number of water molecules around the membrane is correlated to an additional flexibility of PM providing the ability to reach higher thermal fluctuations. The conclusion of this study is that additional water molecules in the proton channel of the triple mutant do not have a similar effect, suggesting that they are closely confined in the protein structure.

The structural differences between the triple mutant and wt are mainly located in the cytoplasmic part of helices E, F, G and the E–F loop and directly concern about one fifth of the BR amino acids. It is possible and cannot be excluded from the present work that local dynamical changes appear in these regions, which are not visible in the average mean square amplitudes of the membrane as a whole, which were explored in our study. The fact that the helices in the mutant take up a different conformation than that in the wt does not necessarily mean that they have different dynamical behaviour such as greater flexibility, for example. It has been reported that helices F and G cause the movement and/or disordering of the nearby lipid molecule, because its density has not been resolved in the triple mutant structure (Subramaniam and Henderson 2000). However, we

might expect the tilt of the helices accompanied by an increase in the inner volume of the protein to lead to lipid-ordering through an increase of the lateral pressure since the lattice parameter remains constant. In either case the lipid–protein arrangement in PM should not gain any flexibility. There may be some evidence of different lipid ordering in the difference Fourier maps of the wt and mutant, but as we pointed out in the Results section it is difficult to provide a reliable interpretation of such features, because of the inherent limitations of the method. The occurrence of local dynamical differences between wt and triple mutant could be investigated by specific deuterium-labelled mutant PM samples similar to the work of Réat et al. (1998). BR dynamics is not homogeneous and neutron scattering experiments, an analysis of Debye–Waller factors in electron and X-ray crystallography, molecular dynamics simulations and low-frequency dynamics studies by solid-state NMR have indicated its asymmetric distribution over the protein and greater flexibility of the cytoplasmic region of BR compared with the rest of the molecule (Belrhali et al. 1999; Grigorieff et al. 1996; Réat et al. 1998; Xu et al. 1995; Kira et al. 2004).

Interestingly, the triple mutant has been shown to be active in proton translocation. It passes a spectroscopic M-state- like intermediate, which does not show large conformational differences with the ground-state structure, and irreversibly decays (as in the wt) back to the initial state (Tittor et al. 2002). Proton pump kinetics and energetics, therefore, are not necessarily associated with large conformational changes. It is important to emphasise, however, the difference between structural similarity and energy equivalence. The wt and triple mutant can be seen as 'different' proteins, with different equilibrium structures in their unilluminated, low-energy, ground states. The fact that the triple mutant protein ground-state structure is similar to the wt M intermediate could be considered as a coincidence, since the wt M state is a 'strained' state, which is achieved only upon a gain of photon energy and which relaxes by thermal exchange as the photocycle proceeds. The triple mutant and the wt ground-state BR structures, on the other hand, are stable conformations in thermal equilibrium. The mutations in the triple mutant simply shift the equilibrium position to a conformation similar to the late wt M-state structure, which is only reached after excitation of BR with photon energy and spontaneously decays back to its ground state, which clearly indicates it has a higher energy level. The same energetic behaviour, i.e. the spontaneous decay back to its ground state, is observed for the triple mutant M state, which has a structure that is highly similar to that of the ground state. We note, therefore, that our neutron scattering experiments investigated a state of similar structure, but not of similar energy. Thermodynamic calculations of the transient late M state compared with the ground state of BR have revealed a loss of entropy and enthalpy (Váró and Lanyi 1991b) and one would expect lower thermal fluctuations in the intermediate state at physiological temperatures. Because of the very short lifetime of the intermediate it is at present difficult to test this hypothesis by experiment. One possible experimental approach is by real time kinetics measurements of M-state dynamics, by using a stroboscopic method to accumulate a significant data set from a sufficient number of equivalent time slices.

Acknowledgements We are grateful to M. Weik and J. Tittor for useful discussions, to J. P. Colletier for a critical reading of the manuscript, and to S. Benkert and S. v. Gronau for preparing wt and triple mutant PM. We thank G. Fragneto-Cusani, S. Wood, B. Frick, O. Losserand, C. Pfister, M. Bée, A. Vandeneyde and the ILL for excellent support during the neutron experiments. This work was supported by Deutsche Forschungsgemeinschaft (SFB533) and EU grant HPRI-CT-2001-50035 on the Improving Human Potential Programme.

References

Belrhali H, Nollert P, Royant A, Menzel C, Rosenbusch JP, Landau EM, Pebay-Peyroula E (1999) Protein, lipid and water organization in bacteriorhodopsin crystals: a molecular view of the purple membrane at 1.9 A resolution. Struct Fold Des 7:909–17

Blaurock AE, Stoeckenius W (1971) Structure of the purple membrane. Nat New Biol 233:152–155

Cao Y, Váró G, Chang M, Ni B, Needleman R, Lanyi JK (1991) Water is required for the proton transfer from aspartate-96 to the bacteriorhodopsin Schiff base. Biochemistry 30:10972–10979

Dencher NA, Dresselhaus D, Zaccai G, Büldt G (1989) Structural changes in bacteriorhodopsin during proton translocation revealed by neutron diffraction. Proc Natl Acad Sci USA 86:7876–9

Dencher NA, Sass HJ, Büldt G (2000) Water and bacteriorhodopsin: structure, dynamics, and function. Biochimica et Biophysica Acta 1460:192–203

Ferrand M, Dianoux AJ, Petry W, Zaccai G (1993) Thermal motions and function of bacteriorhodopsin in purple membranes: effects of temperature and hydration studied by neutron scattering. Proc Natl Acad Sci USA 90:9668–9672

Gabel F, Bicout D, Lehnert U, Tehei M, Weik M, Zaccai G (2002) Protein dynamics studied by neutron scattering. Quat Rev Biophys 35:327–367

Grigorieff N, Ceska TA, Downing KH, Baldwin JM, Henderson R (1996) Electron-crystallographic refinement of the structure of bacteriorhodopsin. J Mol Biol 259:393–421

Haupts U, Tittor J, Oesterhelt D (1999) Closing in on bacteriorhodopsin: progress in understanding the molecule. Annu Rev Biophys Biomol Struct 28:367–99

Henderson R, Unwin PN (1975) Three-dimensional model of purple membrane obtained by electron microscopy. Nature 257:28–32

Henderson R, Baldwin JM, Downing KH, Lepault J, Zemlin F (1986) Structure of purple membrane from *Halobacterium halobium*: recording, measurement and evaluation of electron micrographs at 3.5 Å resolution. Ultramicroscopy 19:147–178

Jubb JS, Worcester DJ, Crespi HL, Zaccaï G (1984) Retinal location in purple membrane of *Halobacterium halobium* : a neutron diffraction study of membranes labelled in vivo with deuterated retinal. EMBO J 3:1455–1461

Kamikubo H, Kataoka M, Váró G, Oka T, Tokunaga F, Needleman R, Lanyi JK (1996) Structure of the N intermediate of bacteriorhodopsin revealed by X-ray diffraction. Proc Natl Acad Sci USA 93:1386–90

Kandori H (2000) Role of internal water molecules in bacteriorhodopsin. Biochemica et Biophysica Acta 1460:177–191

Karplus M, McCammon JA (1983) Dynamics of proteins: elements and function. Ann Rev Biochem 53:263–300

Kates M, Kushwaha SC, Sprott GD (1982) Lipids of purple membrane from extreme halophiles and of methanogenic bacteria methods in enzymology, vol 88. Academic, pp 98–105

Kira A, Tanio M, Tuzi S, Saito H (2004) Significance of low-frequency local fluctuation motions in the transmembrane B and C alpha-helices of bacteriorhodopsin, to facilitate efficient proton uptake from the cytoplasmic surface, as revealed by site-directed solid-state (13)C NMR. Eur Biophys J 33(7):580–588

Kneller GR, Smith JC (1994) Liquid-like side-chain dynamics in myoglobin. J Mol Biol 242:181–185

Koch MH, Dencher NA, Oesterhelt D, Plohn HJ, Rapp G, Büldt G (1991) Time-resolved X-ray diffraction study of structural changes associated with the photocycle of bacteriorhodopsin. Embo J 10:521–526

Lehnert U, Reat V, Weik M, Zaccai G, Pfister C (1998) Thermal motions in bacteriorhodopsin at different hydration levels studied by neutron scattering: correlation with kinetics and light- induced conformational changes. Biophys J 75:1945–1952

Luecke H, Schobert B, Richter HT, Cartailler JP, Lanyi JK (1999) Structure of bacteriorhodopsin at 1.55 A resolution. J Mol Biol 291:899–911

Luecke H, Schobert B, Cartailler JP, Richter HT, Rosengarth A, Needleman R, Lanyi JK (2000) Coupling photoisomerization of retinal to directional transport in bacteriorhodopsin. J Mol Biol 300:1237–1255

Maeda A, Tomson FL, Gennis RB, Kandori H, Ebrey TG, Balashov SP (2000) Relocation of internal bound water in bacteriorhodopsin during the photoreaction of M at low temperature: an FTIR study. Biochemistry 39:10154–10162

O'Brien FEM (1948) The control of humidity by saturated salt solutions. J Sci Instr 25:73–76

Oesterhelt D, Stoeckenius W (1974) Isolation of the cell membrane of *Halobacterium halobium*and its fractionation into red and purple membrane. Methods Enzymol 31(PtA):667–678

Papadopoulos G, Dencher NA, Zaccai G, Büldt G (1990) Water molecules and exchangeable hydrogen ions at the active centre of bacteriorhodopsin localized by neutron diffraction. Elements of the proton pathway?. J Mol Biol 214:15–19

Pebay-Peyroula E, Rummel G, Rosenbusch JP, Landau EM (1997) X-ray structure of bacteriorhodopsin at 2.5 angstroms from microcrystals grown in lipidic cubic phases. Science 277:1676–1681

Réat V, Zaccai G, Ferrand M, Pfister C (1996) Functional Dynamics in Purple Membrane Workshop on Inelastic and Quasielastic Neutron Scattering in Biology, Grenoble

Réat V, Patzelt H, Ferrand M, Pfister C, Oesterhelt D, Zaccai G (1998) Dynamics of different functional parts of bacteriorhodopsin: $H-^{2}H$ labeling and neutron scattering. Proc Natl Acad Sci USA 95:4970–4975

Sass H, Schachowa I, Rapp G, Koch MHJ, Oesterhelt D, Dencher NA, Büldt G (1997) The tertiary structural changes in bacteriorhodopsin occur between M states: X-ray diffraction and Fourier transform infrared spectroscopy. EMBO J 16:1484–1491

Sass HJ, Büldt G, Gessenich R, Hehn D, Neff D, Schlesinger R, Berendzen J, Ormos P (2000) Structural alterations for proton translocation in the M state of wild-type bacteriorhodopsins. Nature 406:649–653

Schobert B, Brown LS, Lanyi JK (2003) Crystallographic structures of the M and N intermediates of bacteriorhodopsin: assembly of a hydrogen-bonded chain of water molecules between Asp-96 and the retinal Schiff base. J Mol Biol 330:553–570

Smith JC (1991) Protein dynamics: comparison of simulations with inelastic neutron scattering experiments. Quart Rev Biophy 24:227–291

Subramaniam S, Henderson R (2000) Molecular mechanism of vectorial proton translocation by bacteriorhodopsin. Nature 406:653–657

Subramaniam S, Lindahl M, Bullough P, Faruqi AR, Tittor J, Oesterhelt D, Brown L, Lanyi J, Henderson R (1999) Protein conformational changes in the bacteriorhodopsin photocycle. J Mol Biol 287:145–61

Tittor J, Paula S, Subramaniam S, Heberle J, Henderson R, Oesterhelt D (2002) Proton translocation by bacteriorhodopsinn in the absence of substantial conformational changes. J Mol Biol 319:555–565

Váró G, Lanyi JK (1990) Pathways of the rise and decay of the M photointermediates(s) of bacteriorhodopsin. Biochemistry 29:2241–2250

Váró G, Lanyi JK (1991a) Kinetic and spectroscopic evidence for an irreversible step between deprotonation and reprotonation of the Schiff base in the bacteriorhodopsin photocycle. Biochemistry 30:5008–50015

Váró G, Lanyi JK (1991b) Thermodynamics and energy coupling in the bacteriorhodopsin photocycle. Biochemistry 30:5016–5022

Váró G, Lanyi JK (1995) Effects of Hydrostatic Pressure on the Kinetics Reveal a Volume Increase during the Bacteriorhodopsin Photocycle. Biochemistry 34:12161–12169

Vonck J (2000) Structure of the bacteriorhodopsin mutant F219L N intermediate revealed by electron crystallography. Embo J 19:2152–2160

Weik M, Patzelt H, Zaccai G, Oesterhelt D (1998a) Localization of glycolipids in membranes by in vivo labeling and neutron diffraction. Mol Cell 1:411–419

Weik M, Zaccai G, Dencher NA, Oesterhelt D, Hauss T (1998b) Structure and hydration of the M-state of the bacteriorhodopsin mutant D96N studied by neutron diffraction. J Mol Biol 275:625–634

Xu D, Sheves M, Schulten K (1995) Molecular Dynamics Study of the M_{412} Intermediate of Bacteriorhodopsin. Biophys J 69:2745–2760

Zaccai G (1987) Structure and hydration of purple membranes in different conditions. J Mol Biol 194:569–572

Zaccai G (2000) How soft is a protein? A protein dynamics force constant measured by neutron scattering. Science 288:1604–1607

Zaccai G, Gilmore DJ (1979) Areas of hydration in the purple membrane of *Halobacterium halobium*: a neutron diffraction study. J Mol Biol 132:181–191

Zamyatin AA (1972) Protein volume in solution. Prog Biophys Mol Biol 24:107–123